ACADEMIC PRESS

Available online at www.sciencedirect.com

SCIENCE DIRECT®

Journal of Magnetic Resonance 159 (2002) 207–212

JMR Journal of Magnetic Resonance

www.academicpress.com

RIDE'n RIPT—ring down elimination in rapid imaging pulse trains☆

Klaus Woelk,[a,*] Peter Trautner,[a] Heiko G. Niessen,[a] and Rex E. Gerald II[b]

[a] *Institute of Physical and Theoretical Chemistry, University of Bonn, Wegelerstrasse 12, D-53115 Bonn, Germany*
[b] *Chemical Technology Division, Argonne National Laboratory, 9700 South Cass Avenue, Argonne, IL 60439, USA*

Received 21 June 2002; revised 4 October 2002

Abstract

A new pulse sequence is introduced for compensation of acoustic ringing effects, which occur in rotating-frame images obtained with the rapid imaging pulse trains (RIPT). The new sequence (RIDE'n RIPT) combines features of ring down elimination (RIDE), the most common difference-spectroscopy sequence for acoustic-ringing compensation, with the advantages of RIPT for fast acquisition of magnetization profiles in B_1 field gradients. For even greater time efficiency in many experiments, the two transients of RIDE'n RIPT are combined to a single transient in which data for the difference spectroscopy are collected sequentially. RIDE'n RIPT was used to record one-dimensional profiles of the proton magnetization in supercritical fluid samples of methane in carbon dioxide. The profiles showed substantial improvements over profiles obtained from standard RIPT. To withstand the high pressures required for the supercritical carbon dioxide mixtures, a toroid cavity autoclave (TCA) was used as the NMR resonator and pressure vessel. The well-defined, strong, and nonuniform B_1 field of the TCA was used to resolve distances along the radial dimension.

Keywords: Acoustic ringing; RIDE; RIPT; Rotating-frame imaging; Radiofrequency gradient; Toroid cavity; High-pressure probe

1. Introduction

The application of radiofrequency (rf) pulses to NMR resonators (coils or cavities) causes alternating currents in the resonance circuitry and generates rf magnetic fields (B_1) that induce additional currents (eddy currents) in nearby metallic structures. These structures may be the probe housing, electronic parts, or parts of the sample if it is metallic. In the presence of a static magnetic field (B_0), alternating or eddy currents can produce mechanical vibrations in the metal at a frequency about that of the imposed NMR pulse. A reciprocal process generates an rf signal that is detected by the resonator [1,2]. This transient response to the action of an NMR pulse is known as "acoustic ringing" (AR) and, although AR relaxes within tens of microseconds, it often causes baseline distortions that are especially noticeable in the spectra of weak or short FIDs. Among the several techniques to suppress AR, or compensate for it [2–7], delayed FID acquisition is standard in high-resolution liquid NMR, and difference spectroscopy is common if the duration of the FID is of the order of the AR decay, e.g., in solid-state NMR [3] or in specialized solution NMR such as ^{17}O spectroscopy [4,5].

An area where AR is a particularly significant problem is multiple pulse NMR experiments with interpulse data acquisition. The interpulse spacing can be as short as a few microseconds, and is determined by a desired spectral window. In particular, the cyclic sequences WAHUHA and MREV-8 [8] for homonuclear decoupling in solid-state NMR are conducted this way, as is rapid imaging pulse trains (RIPT, Fig. 1) for rapid rotating-frame imaging [9–11]. In these multiple pulse

☆ The submitted manuscript has been created in part by the University of Chicago as Operator of Argonne National Laboratory ("Argonne") under Contract No. W-31-109-ENG-38 with the US Department of Energy. The US Government retains for itself, and others acting on its behalf, a paid-up, nonexclusive, irrevocable worldwide license in said article to reproduce, prepare derivative works, distribute copies to the public, and perform publicly and display publicly, by or on behalf of the Government.

* Corresponding author. Fax: +49-228-73-9424.
E-mail address: woelk@thch.uni-bonn.de (K. Woelk).

1090-7807/02/$ - see front matter © 2002 Elsevier Science (USA). All rights reserved.
PII: S1090-7807(02)00105-2

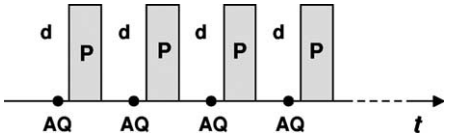

Fig. 1. Rapid imaging pulse train (RIPT) for recording nutation interferograms. Single data points are acquired (AQ) between the application of two hard pulses (P).

techniques, one or more rf pulses precede each single data point acquisition, and AR perturbs all data points equally. This is in contrast with standard FID acquisition where only those data points are effected that were recorded within the decay of the AR from the observe pulse. Accordingly, delay of acquisition to after the AR decay works well in high-resolution liquid NMR but cannot be applied to multiple pulse techniques in which the interpulse spacing is short compared to the AR decay.

Several calculation methods such as backward linear prediction have been suggested, in which the perturbed early part of the FID is recalculated with help from later parts that are undisturbed by AR. These calculation methods have been reviewed in [2]; however, all of them rely on an undisturbed later part of the FID to recalculate or extract information from the early part. Consequently, calculation methods fail when all data points are equally effected by AR as exemplified for the multiple pulse techniques.

The compensation of ring down effects with difference spectroscopy is based on the reproducibility of AR and its sensitivity to the phase of the preceding rf pulse. In the two consecutive transients of ring down elimination (RIDE) [6], the most common difference spectroscopy for AR compensation, magnetization is brought to the same position in the rotating frame of reference using rf pulses of opposite transmitter phase. An FID is acquired after each of the two transients and, because only ring down resonances are rf phase sensitive, the sum of the two FIDs cancels AR but co-adds intensities from the sample magnetization. The two transients of RIDE are often obtained from the pulse sequences (90° – AQ) and (180° – [–90°] – AQ), where AQ denotes the FID acquisition. However, a more general sequence is exemplified in Fig. 2, in which an arbitrary pulse width P_1 is applied rather than just the 90° pulse width. Consequently, RIDE is also applicable to NMR experiments with the nonuniform B_1 fields of surface coils or toroid cavity detectors (TCDs, [12,13]), for which no common single-pulse nutation angle (flip angle) is determined.

2. Acoustic ringing in TCDs

The TCD is a cylindrical cavity resonator that confines the B_1 field to the inside of the resonator. Accordingly, unlike in the more common coil geometries of solenoid or Helmholtz coils, no fringe field exists about a TCD, and no eddy currents are induced in metallic structures in the vicinity of the TCD. In addition, only the alternating currents in the top and the bottom of a TCD are perpendicular to B_0 and, thus, generate AR [7]. A TCD that is incorporated into a metal pressure vessel [12] or built as a toroid cavity autoclave (TCA, [14]) is well-suited for NMR investigations of gas or fluid systems under high pressure. Especially, supercritical CO_2 ($scCO_2$) has been utilized many times for in situ NMR investigations with TCDs or TCAs to elucidate the CO_2's quality as a modern, environmentally benign, and highly diffusive reaction medium for hydrogenation and hydroformylation catalysis [13–15]. Fig. 3 shows 200 MHz ^{1}H TCA spectra of methane (partial pressure of 3 bar) in $scCO_2$ at 100 bar and 40 °C, which were recorded with a pre-acquisition delay of only 5 μs. Spectrum **a** (Fig. 3) was obtained after a simple single-pulse excitation and exhibits a very intense and broad resonance from TCD AR in addition to the narrow methane signal. In Spectrum **b**, AR effects are compensated with RIDE, so that the baseline is nearly flat.

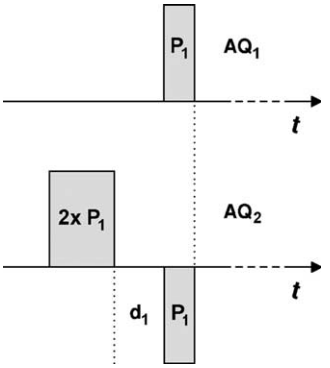

Fig. 2. Ring down elimination (RIDE) through difference spectroscopy. Because acoustic ringing is sensitive to the phase of the rf pulses (P_1), the sum of AQ_1 and AQ_2 cancels ring down effects but co-adds intensities from sample magnetization.

In addition to the high-pressure capabilities, TCDs and TCAs are also useful for obtaining radially resolved magnetization profiles with rotating-frame imaging (RFI). In the vicinity of the central conductor of TCDs and TCAs, RFI achieves spatial resolutions down to the micrometer scale along the radial dimension [16]. In the traditional, chemical-shift-resolved RFI, a series of FIDs is recorded with incrementally increasing pulse widths. The pulse-width dependent FIDs are Fourier transformed two-dimensionally leading to intensities as a function of chemical shift in f_2 and radial distance from the center axis of the torus in f_1. Alternatively, the time-saving RIPT technique (Fig. 1)—RIPT takes only milliseconds of experimental time—provides for nutation interferograms that, after a sine Fourier transfor-

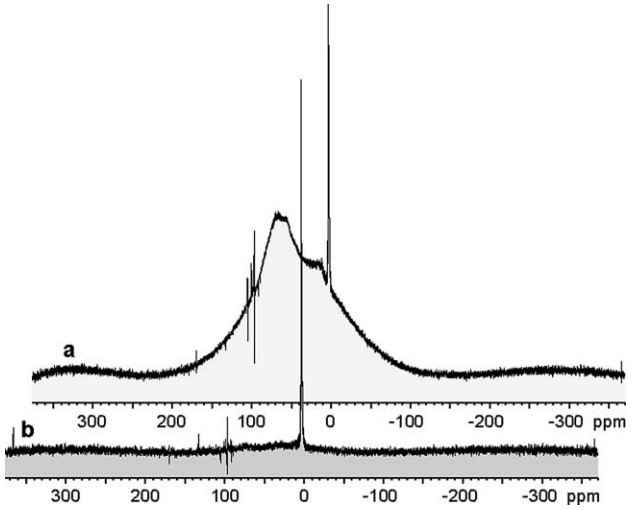

Fig. 3. Spectra of methane (partial pressure of 3 bar) in $scCO_2$ (100 bar, 40 °C) obtained from a toroid cavity autoclave (TCA) with the pulse width (P_1 in Fig. 2) set to the maximum-intensity pulse width according to [12]. The pre-acquisition delay between P_1 and the acquisition of the first FID data point was 5 μs. (a) Single-pulse excitation, (b) RIDE difference spectroscopy ($d_1 = 1$ μs).

mation and appropriate scaling, result in radially resolved magnetization profiles. In the magnetization profiles of RIPT, chemical-shift information is not resolved.

Because AR equally perturbs all data points from the multiple pulse experiment RIPT, a pre-acquisition delay of up to 100 μs must be applied before the acquisition of a each data point. Since typical values for the RIPT pulse width and the single-point acquisition time are 10 and 0.2 μs, respectively, the experimental time of RIPT is usually dominated by the pre-acquisition delay to avoid AR. To obtain magnetization profiles with maximum spatial resolution and optimum sensitivity even in highly diffusive or fast relaxing media, it is important to minimize the effects of diffusion and relaxation during the pulse sequence. Consequently, it is primarily desirable to minimize the delays in the RIPT sequence. Fig. 4 shows ^1H radial profiles at a resonance frequency of 200 MHz obtained with RIPT from the TCA filled with either (a) pure $scCO_2$ (100 bar, 40 °C, no detectible proton signal) or (b) methane (partial pressure of 3 bar) in $scCO_2$ (100 bar, 40 °C). The pre-acquisition delays in our experiments (Fig. 4) were set to only 5 μs, and severe acoustic-ringing distortions render it impossible to evaluate the profiles quantitatively. Especially, the upper profile shows significant spatial structure even though it was recorded from a sample of no protons. It appears that the intensity of these structures increases as the radial distance in the TCA decreases, i.e., the AR distortion is at maximum close to the central conductor (inner sample boundary of 0.8 mm). However, because spin density data are generated from scaling raw intensities with

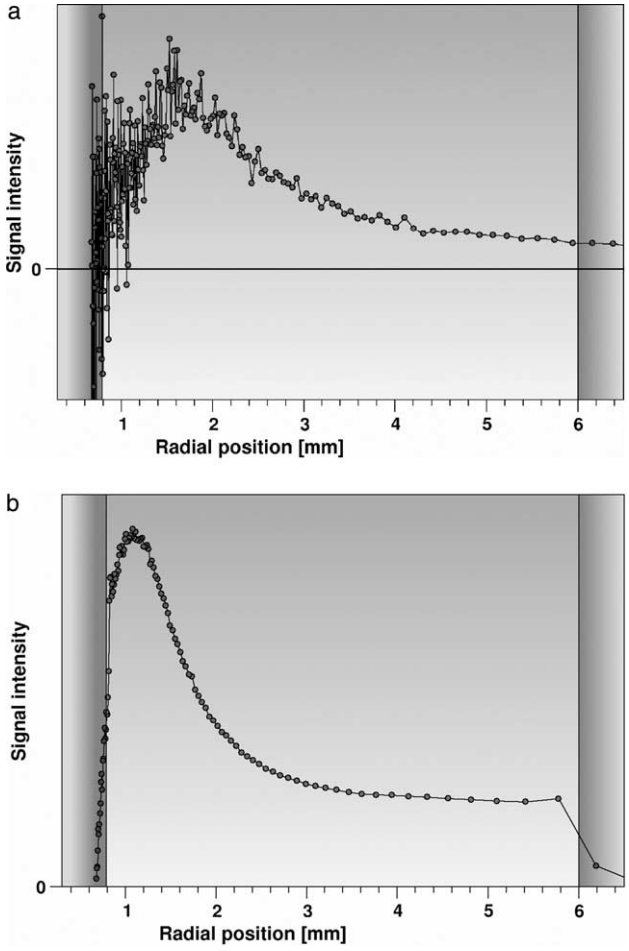

Fig. 4. RIPT profiles obtained from a TCA filled with (a) pure $scCO_2$ (100 bar, 40 °C) and (b) methane (partial pressure of 3 bar) in $scCO_2$ (100 bar, 40 °C). Severe profile distortions from acoustic ringing are visible in both profiles. The ordinate scale (signal intensity) of (a) is enlarged 15 times compared to (b). Both spectra were obtained without averaging (200 MHz ^1H transmitter power of 100 W) from a single transient of 512 RIPT pulses of 10 μs (P in Fig. 1) with data acquisition during 5 μs interpulse delays (d in Fig. 1). The TCA's sample dimensions were 0.8 mm (inner radius), 6.0 mm (outer radius), and 20 mm (height). The radial sample boundaries are visualized by the vertical bars.

$1/r^2$, where r is the radial position, i.e., the distance from the center axis of the TCA [12], the effects from AR are overemphasized at small r. Because of the same scaling procedure, noise increases substantially with decreasing r in the radial profiles, which is especially visible in Fig. 4a in which the signal intensity axis is enlarged 15 times compared with Fig. 4b. All efforts failed to eliminate AR effects from the TCA radial profiles by mathematical treatment of the intensity data either before or after the application of the spin-density scaling.

To offset the effects of AR in the multiple pulse imaging technique RIPT, we developed a combination of RIPT with the compensating difference spectroscopy

RIDE. In this interleaved RIDE'n RIPT combination, a RIDE sequence precedes the acquisition of each data point.

3. The RIDEn RIPT sequence

The two transients of RIDE'n RIPT are shown in Fig. 5, in which two RIDE pulses precede the acquisition of each single data point. Different from the original sequence (Fig. 2), the RIDE part in Fig. 5 consists of two pulses for both transients, which are identical in width but phase shifted by 180°. Accordingly, the time frames of the two transients are exactly synchronized. During RIDE, magnetization is moved away from, but then returned to, its original location in the rotating frame of reference. Consequently, no net effect occurs for the sample magnetization if the RIDE pulses and the interpulse delays d_1 are sufficiently short (e.g., $P_1 = 10\,\mu s$, $d_1 = 1\,\mu s$) and, thus, off-resonance and relaxation effects are practically negligible during RIDE. Because the phases of the RIDE pulses for the first transient are opposite to the phases for the second transient, the magnetization is brought to its original location from opposite directions. Accordingly, RIDE'n RIPT provides for an efficient compensation of AR and minimizes the time requirement between the RIPT propagation pulses (P_2). For example, if the delays d_1 are negligible ($d_1 \leqslant 1\,\mu s$, the time required for obtaining a data point (i.e., the acquisition delay) is $d_2 = 3\,\mu s$, and a pulse width of $P_1 = 10\,\mu s$ is used for RIDE, the time between RIPT pulses is reduced to less than one-fourth of the pre-acquisition delay of $P_2 = 100\,\mu s$ that is routinely applied in TCAs to avoid the effects of AR in standard RIPT experiments. The reduction of the pulse sequence time requirement is especially important for imaging diffusion and relaxation phenomena (diffusiometry and relaxometry, respectively) in which the effects of diffusion and relaxation during the pulse and acquisition periods are neglected in the mathematical treatment [17]. However, the energy delivered to the sample by the RIDE'n RIPT sequence is three times larger than in the conventional RIPT. While this is not a serious concern for nonconducting samples, increased rf heating must be considered in conducting samples or in vivo applications.

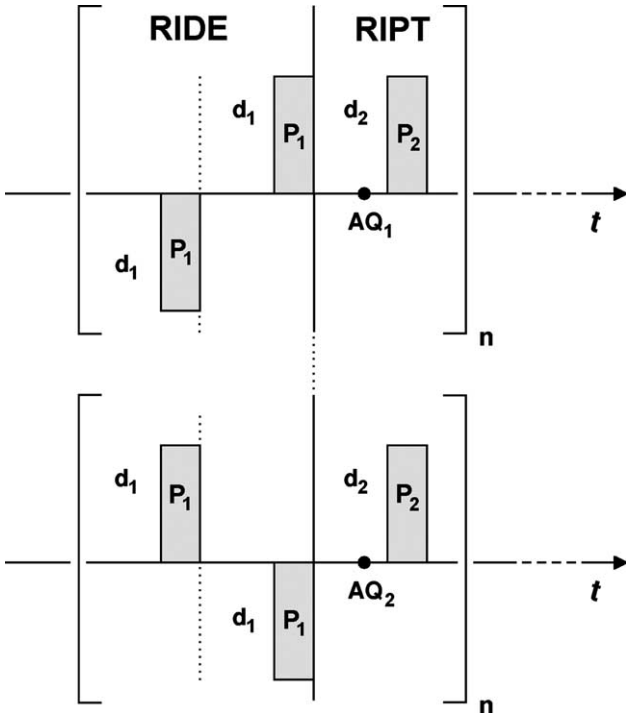

Fig. 5. Ring down elimination in rapid imaging pulse trains (RIDE'n RIPT). A RIDE sequence precedes the acquisition of every single data point AQ_1 and AQ_2, so that the sum of AQ_1 and AQ_2 cancels ring down effects but co-adds intensities for the magnetization profile. P_1, RIDE pulses; P_2, RIPT propagation pulse; d_1, RIDE interpulse delay; d_2, pre-acquisition delay.

Fig. 6 shows spectra from the samples of Fig. 4 recorded with the new RIDE'n RIPT difference spectroscopy. AR effects are reduced so much that the homogeneous distribution of methane in $scCO_2$ becomes clearly visible in the lower profile, and only thermal noise that increases substantially with decreasing r is recorded in the upper profile of no protons (pure $scCO_2$). For comparison, the profiles of Fig. 4 are added equally scaled in light gray to the plots of Fig. 6.

In some of our experiments—especially when the RIPT propagation pulse width P_2 was very short—, ring down elimination was not complete with the RIDE pulses set to $P_1 = P_2$. In these cases, we extended P_1 independently of P_2 until complete compensation was achieved. If, however, AR compensation is sufficient with $P_1 = P_2$, the two transients of RIDE'n RIPT may be combined to a single transient as shown in Fig. 7. The nutation interferograms that were recorded in two transients before are now collected sequentially within one transient. By comparison of Fig. 7 with Fig. 5, it is easy to identify how the two transients are interleaved in the new sequence. Accordingly, AQ_1 delivers data points for the first and AQ_2 for the second transient. Subsequent to the experiment, the interleaved nutation interferograms AQ_1 and AQ_2 are separated and processed like those of Fig. 5. For appropriate AR compensation of the first data point, it is important that the acquisition loop is preceded by two separate pulses P_1 with opposite phase as depicted in Fig. 7. A distinct advantage of the combined sequence is a factor of 2 reduction in time with respect to signal-to-noise ratio or, equivalently, a factor of $\sqrt{2}$ improvement in signal to noise with respect to experimental time. In contrast, however, the time frames of the two data

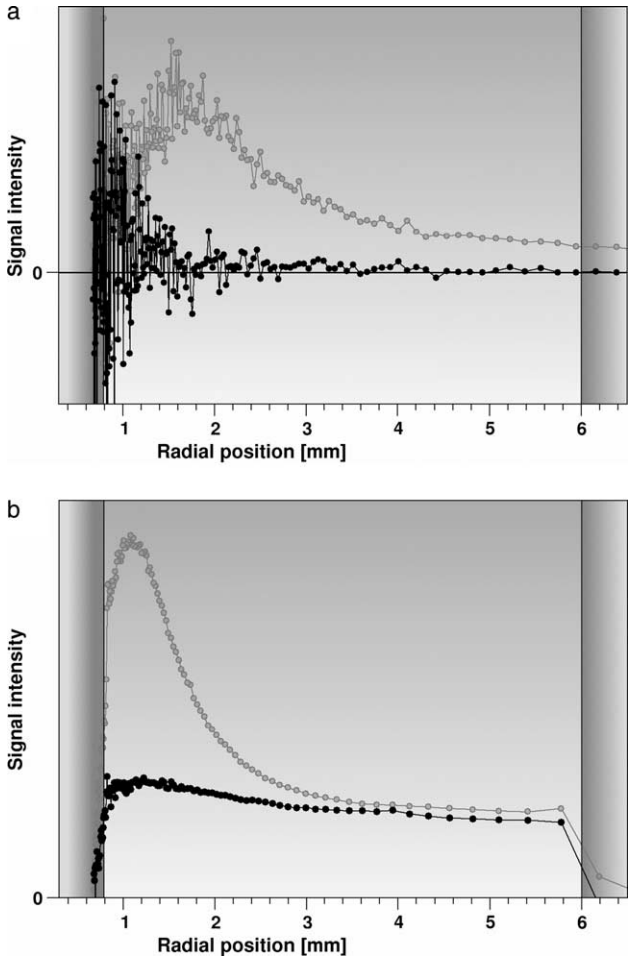

Fig. 6. RIDE'n RIPT profiles ($d_1 = 1\,\mu s$, $d_2 = 5\,\mu s$, and $P_1 = P_2 = 10\,\mu s$) obtained from the same samples and the same TCA of the experiments in Fig. 4, (a) pure $scCO_2$ (100 bar, 40 °C) and (b) methane (partial pressure of 3 bar) in $scCO_2$ (100 bar, 40 °C). The ordinate scale (signal intensity) of (a) is enlarged 15 times compared to (b) and the RIPT profiles of Fig. 4 are shown in light gray for comparison.

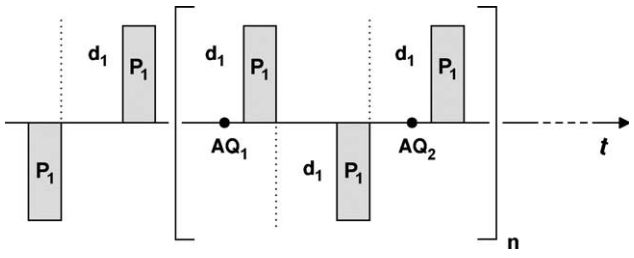

Fig. 7. Combined RIDE'n RIPT sequence for recording AQ_1 and AQ_2 sequentially in a single transient. The acquisition loop conducted n times is preceded by two pulses with opposite phase, and all pulse widths are identical (P_1).

sets AQ_1 and AQ_2 are slightly shifted versus each other, which sometimes leads to insufficient ring down elimination or additional artifacts from diffusion or relaxation.

Acknowledgments

This work was supported by the Deutsche Forschungsgemeinschaft (DFG) under Program WO 613/2-2 and in part by the US Department of Energy, Division of Chemical Sciences, Office of Basic Energy Sciences, under Contract W-31-109-Eng-38. H.G.N. thanks the Studienstiftung des deutschen Volkes for a research fellowship, R.E.G. thanks the DFG collaborative research center SFB 334 for a travel grant to visit the University of Bonn in Germany, during which this work was initiated.

References

[1] E. Fukushima, S.B.W. Roeder, Spurious ringing in pulse NMR, J. Magn. Reson. 33 (1979) 199–203.
[2] I.P. Gerothanassis, Methods of avoiding the effects of acoustic ringing in pulsed Fourier transform nuclear magnetic resonance spectroscopy, Prog. NMR Spectrosc. 19 (1987) 267–329.
[3] G. Neue, C. Dybowski, M.L. Smith, D.H. Barich, Fitting of low-intensity wide-line spectra dominated by chemical shift anisotropy, Solid State NMR 3 (1994) 115–119.
[4] I.P. Gerothanassis, J. Lauterwein, An evaluation of various pulse sequences for the suppression of acoustic ringing in oxygen-17 NMR, J. Magn. Reson. 66 (1986) 32–42.
[5] A. Bagno, A pulse sequence for T_1 measurements by inversion-recovery in the presence of acoustic ringing, Magn. Reson. Med. 30 (1992) 1164–1168.
[6] P.S. Belton, I.J. Cox, R.K. Harris, Experimental sulphur-33 nuclear magnetic resonance spectroscopy, J. Chem. Soc., Faraday Trans. 2 81 (1985) 63–75.
[7] R.E. Gerald II, L.H. Nuñez, J.W. Rathke, Nuclear magnetic resonance detector used for reducing probe ringing, US patent 6,191,583, issued February 20, 2001.
[8] K. Schmidt-Rohr, H.W. Spiess, in: Multidimensional Solid-State NMR and Polymers, Academic Press, London, 1994, pp. 72–77.
[9] K.R. Metz, J.P. Boehmer, Technique for rapid rotating-frame imaging, Magn. Reson. Imag. 6 (Suppl. 1) (1988) 53.
[10] D. Boudot, D. Canet, J. Brondeau, Spatial labeling by a radiofrequency field gradient. DANTE-Z profile, probed by one-dimensional nutation imaging, J. Magn. Reson. 87 (1990) 385–394.
[11] K.R. Metz, J.P. Boehmer, J.L. Bowers, J.R. Moore, Rapid rotating-frame imaging using an rf pulse train (RIPT), J. Magn. Reson. B 103 (1994) 152–161.
[12] K. Woelk, J.W. Rathke, R.J. Klingler, The toroid cavity NMR detector, J. Magn. Reson. A 109 (1994) 137–146.
[13] J.W. Rathke, R.J. Klingler, R.E. Gerald II, K.W. Kramarz, K. Woelk, Toroids in NMR spectroscopy, Prog. NMR Spectrosc. 30 (1997) 209–253.
[14] H.G. Niessen, P. Trautner, S. Wiemann, J. Bargon, K. Woelk, The toroid cavity autoclave for high-pressure and variable-temperature in situ NMR studies, Rev. Sci. Instrum. 73 (2002) 1259–1266.
[15] J.W. Rathke, R.J. Klingler, R.E. Gerald II, K.W. Kramarz, K. Woelk, Toroids in NMR Spectroscopy, Prog. NMR Spectrosc. 30 (1997) 209–253.
[16] J.W. Rathke, R.J. Klingler, R.E. Gerald II, D.E. Fremgen, K. Woelk, S. Gaemers, C.J. Elsevier, NMR spectroscopy, in: P.G.

Jessop, W. Leitner (Eds.), Chemical Synthesis using Supercritical Fluids, Wiley-VCH, Weinheim, 1999, pp. 165–194.

[17] K. Woelk, J.W. Rathke, R.J. Klingler, Rotating-frame NMR microscopy using toroid cavity detectors, J. Magn. Reson. A 105 (1993) 113–116.

[18] K. Woelk, B.L.J. Zwank, P. Trautner, E. Lehnhof, J. Bargon, R.J. Klingler, R.E. Gerald II, J.W. Rathke, Finite-difference approach for the high-precision analysis of rotating-frame diffusion images, J. Magn. Reson. 145 (2000) 276–290.